World Conference on Timber Engineering Oslo 2023

MODE I TESTS OF NORWAY SPRUCE USING SEN-TPB: DETAILED ANALYSIS OF THE CRACK LENGTH DETERMINED USING OPTICAL METHOD

Martin Hataj[1], Jiří Kunecký[2], Michal Kloiber[3]

ABSTRACT: The paper deals with characterization of fracture properties of Norway spruce using SEN-TPB test. Although the matter is not new, methods of processing the results are relatively recent. The article focuses on determination of crack length using DIC, however, the core of the work is the algorithm which determines the crack length based on the correlated point data. Results of optical measurement are compared to compliance-based analytical formulas. Altogether 18 experiments in radial orientation have been made. Samples used for determination of the strain energy release rate were 60 mm in width and 120 mm in height. Wider specimens have been used to employ the orientation of anatomical directions of the tested timber. Two cameras were used to track cracks on both sides. The algorithm works well, although interesting questions arise, especially when we look at the crack length determination algorithm and its failure criteria.

KEYWORDS: SEN-TPB, Norway spruce, digital image correlation, strain energy release rate, crack length

1 INTRODUCTION

Energy-based methods, especially cohesive zone modelling or LEFM provide us with solutions for problems, which are problematic to solve using standard stress-based approaches. Such methods are crucially dependent on proper material properties characterization, especially strain energy release rate [1]. This quantity is, however, highly dependent on mode (or combination of modes) under which the material is loaded. This article deals with mode I, as it is the most common and easiest one to perform. There is a lot of literature about mode I testing and Norway spruce (as a typical softwood) which is also an advantage, since one can easily compare the results to the previously published values. In all quasi-brittle materials, including timber, there exists some kind of size effect [2], which has to be taken into account. That is also the reason why authors did not choose narrow and rather low sample size used in the previously published works [3,4]. Of course, for proper size effect description there is a need of many more experiments and configurations, nevertheless, just repetition of what has been done was not preferred. Also, it is clear that the orientation of anatomical directions of wood is important. The article shows result of radial direction of timber.

Digital image correlation is a method, which is highly suitable to study timber engineering problems, since relatively low values of stiffness of wood allows for good precision of results. Its drawbacks are, of course, that the abundant number of data have to be understood and reinterpreted. This was the most important part of the work, how to get the crack length using experimental data only. Although in the literature there exists a plethora of algorithms [7-9], there is missing an easy criterion to recognize the presence of a crack. Since we see in optical solution relative distance or deformation of two points, it is relatively tricky to say the threshold value to be used to evaluate the crack length properly.

The strain energy release rate is a quantity, which is usually computed using one of the compliance-based methods. Its advantage is that is does not require complicated tracking of crack length. In the literature e.g. Dourado et al. [1,3], the processing of the data is based on compliance change of the whole specimen, which looks robust, however, it has to be taken into account, that the procedure itself is not purely experimental, since it incorporates also an analytical model, which needs material properties to be inserted and which are only assessed using the initial compliance, which is often tricky due to nonlinearities present in the beginning of the experiment. Another question arises, that the algorithm uses complicated computation of equivalent crack length, which one is complicated to understand and which has to be solved numerically. Last, there is a coefficient k representing the influence of SRR width, which is based on a separate numerical model, thus producing values, which are not directly related to the measured values. Although all criticisms are possible, still it is very robust method.

[1] Martin Hataj, Czech Technical University in Prague, University Centre for Energy Efficient Building, Czech Republic, martin.hataj@cvut.cz
[2] Jiří Kunecký, Institute of Theoretical and Applied Mechanics, Czech Academy of Sciences, Czech Republic, kunecky@itam.cas.cz
[3] Michal Kloiber, Institute of Theoretical and Applied Mechanics, Czech Academy of Sciences, Czech Republic, kloiber@itam.cas.cz

https://doi.org/10.52202/069179-0022

During processing the data and the results the authors have noticed, that the processing of the data is not just a research task, but that it can be educational not only for the authors themselves, but that it is a nice example to help understand the complicated nature of fracture mechanics and eqLEFM especially [2, 6]. Such an approach, where all nonlinear behavior is directly related to a virtual equivalent crack is the simplification, which allows to construct a R-curve and makes understandable the complicated phenomena appearing near crack tip, mainly micro-cracking and fiber-bridging, but also plasticity etc. All the nonlinearities are present in the optical measurement.

2 METHODS

2.1 Samples

The work followed the methods well described in [3], called SEN-TPB, which is basically a three-point bending with glued-in (PVA based dispersions of one-component adhesive) middle part (see Figure 1), where the orientation of grain is rotated 90° to the original one. Dimensions of the samples were chosen 60 mm width and 120 mm height, length 840 mm. In this scale we have already the problem of annual rings, which have slightly rounded shape. This problem can add additional noise to the data. The studied timber was dried using a special protocol in order to simulate conditions present in construction timber: the green wood dried for three months in the forest after harvest and later dried artificially for 14 days to reach the final MC of 12% abs. This could be the way how to let the internal stresses induced by drying at a level commonly found in standard structural timber. The density of the specimens was measured in the range between 429 and 529 kg/m^3 with an average value of 477 kg/m^3.

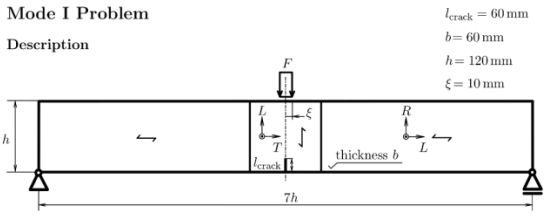

Figure 1: *Description of SEN-TPB test used in the article*

2.2 Loading

The force application was made using a steel plate to spread the loading and avoid shear loading due to misalignment; the supports were made using steel plates and valves to assure free move and omit embedment. When testing a component, usually in the first loading stage one experiences few peaks due to loading all the possible interfaces which are present. This actually happened also here and that was the reason to use curve fitting to the measured force. The test was driven using displacement control, this is important to understand the R-curve. The loading speed was chosen to cause damage in 8-10 minutes.

During the load test, the universal testing machine Galdabini Quasar 100 was used, equipped with a load cell with a range of 10 kN. The outputs from the test machine were processed by the Labtest test software. Furthermore, the DEWE2602 measuring center was used, which is designed to measure the static and dynamic behavior of monitored objects. The microcomputer built into the central unit automatically balances the connected sensors, calibrates the amplifier, and operates the individual measured points in the measurement mode. For each sensor, its constant K is entered, so that the measured values are then directly reported in the exact physical units of the monitored quantities. During the described test, the control panel was controlled by a computer and the DeweSoft program. For all samples, the load value of the joint and the corresponding deflection and path during the initiation and opening of the crack were monitored. Deflection and path during crack initiation and opening were measured by inductive LVDT sensors Micro-epsilon, type DTA-5G-CA throughout the duration of the load test, located on both sides of the test specimen. The average value of these LVDT sensors was used to evaluate the data.

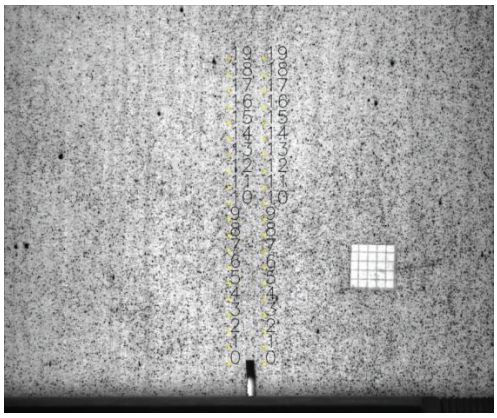

Figure 2: *20 points whose relative displacement was used as an input to the algorithm*

2.3 Compliance-based evaluation

Results were evaluated according to Dourado et al. [3]:

$$E_{Tf} = \left(\frac{L_2^3 - L_1^3}{bH^3} + \frac{L^3 - L_2^3}{b(H - ka_0)^3}\right)\left(\frac{C_0}{2} - \frac{L_1^3}{E_L bH^3}\right)^{-1} \quad (1)$$

where E_{Tf} = corrected value of the flexural modulus, L_1 = lateral arm length (distance between support and nearest glued surface, L_2 = distance between middle of span and support minus side of rectangular SRR – stress relief region (ka), L = distance between middle of span and support, C_0 = initial value of corresponding measured specimen compliance; b = specimen width, H = specimen hight, k = non-dimensional parameter (authors used k = 0,86), a_0 = initial value of the crack length, E_L = the Young's modulus on the longitudinal direction.

https://doi.org/10.52202/069179-0022

$$a_e = \frac{1}{k}\left\{H - \left[\left(\frac{C}{2} - \frac{L_1^3}{E_L b H^3} - \frac{L_2^3 - L_1^3}{E_{Tf} b H^3}\right)^{-1} \frac{L^3 - L_2^3}{E_{Tf} b}\right]^{1/3}\right\} \quad (2)$$

Where a_e = the equivalent crack length, C = specimen compliance (C = δ/P), δ = Castigliano theorem, P = load.

Fracture energy can be obtained by means of the Irwin–Kies equation:

$$G_I = \frac{P^2}{2b}\frac{dC}{da} \quad (3)$$

Equation of the specimen compliance:

$$C = 2\left(\frac{L_1^3}{E_L b H^3} + \frac{L_2^3 - L_1^3}{E_T b H^3} + \frac{L^3 - L_2^3}{E_T b (H - ka)^3}\right) \quad (4)$$

Where E_T = the Young modulus on the transverse direction.

applied to Eq. (3), which leads to:

$$G_I = \frac{3P^2}{b^2}\frac{(L^3 - L_2^3)k}{E_{Tf}(H - ka_e)^4} \quad (5)$$

The initial compliance was set usually between 0.15 and 0.35 times F_{max}. To avoid peaks the curves (force, displacement) were smoothed using moving average filter.

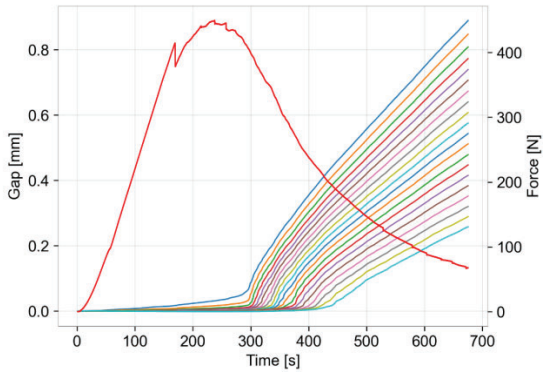

Figure 4: *20 pairs of points (0-9) and their relative displacement show the nonlinear behaviour; measured force in red*

2.4 Optical measurement

The whole test has been recorded with two Basler acA2440-20gm cameras from both sides with a frame rate at 1 Hz and a telecentric lens having 55 mm focal length. The cameras were synchronized using IP protocol and triggered using software trigger from the computer. The camera region of interest was set to not only the crack itself, but also a relatively long path has been recorded using the cameras (see Fig. 2). To ensure we know the ratio (size) of a pixel in distance units, a millimeter scale was glued onto the sample. Synchronization between the optical measurement and loading was made using minimization of error afterwards between the curves of optical displacement in y-direction and displacement measured. Pattern was applied using acryl black and white colors and an airbrush (Revell Masterclass), to meet the standard criterion (3-4 pixels/speckle).

The DIC part consisted of a) tracking several pairs of points (see Figure 2 and 3) using DICe correlation engine [10] and b) based on the data we introduced an algorithm to get the crack length distance.

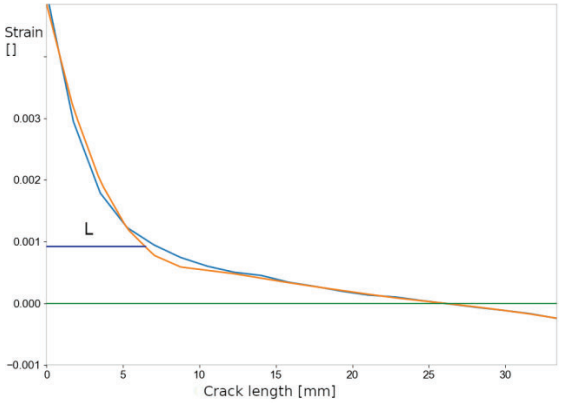

Figure 5: *Crack length determination, crack axis is now the horizontal one. L is the length determined when strain is equal 0.925e-3. Blue is the original data, orange curve is interpolated using polynomial.*

2.4.1 Crack length algorithm

The basic idea of eqLEFM: if there is some nonlinearity (change of compliance) present in the force-displacement curve, it means some length of virtual or equivalent crack is produced; we do not know exactly what happens in the region, however, we look at solution of equation:

$$U = 2\left[\int_0^{L_1} \frac{M_f^2}{2E_L I} dx + \int_{L_1}^{L_2} \frac{M_f^2}{2E_T I} dx + \int_{L_2}^{L} \frac{M_f^2}{2E_T I_{ST}} dx\right] \quad (6)$$

Where U = strain energy due to bending, M_f = the bending moment ($M_f = Px/2$), I = the second moment of area of the entire section (height H), I_{ST} = the second moment of area of the effective section in the SRR (height of H - ka).

$$I = \frac{bH^3}{12} \quad (7)$$

$$I_{ST} = \frac{b(H - ka)^3}{12} \quad (8)$$

Using Castigliano theorem:

$$\delta = \frac{\partial U}{\partial P} \quad (9)$$

We can evaluate compliance (4) and using (3) also G_I. This solution means in fact, that every change in the whole system will lead to change of equivalent crack length,

https://doi.org/10.52202/069179-0022

although it is not still apparent or visible. This is, however, not possible in direct experimental way – the FPZ region and nonlinearity at the crack tip do not allow for this. The biggest disadvantage is, that the most important parameter we want to assess, the resistance to crack growth at the ultimate load (G_c) is in this nonlinear region, not in the one, where the crack is already visible by naked eye, where the curve of loading already turns down.
The algorithm used for evaluation of the optical measurement cannot follow the same approach, however, it can try to do similar technology – recognize the crack as a threshold value of linear behavior between a pair of correlated points. In steps:

1. In each moment (time) we can plot the point difference divided by their original distance (see Fig. 2 and 5)
2. Stabilize the curve (in each step the curve is moving a bit) - smooth it using a curve (here we used piecewise cubic Hermite interpolating polynomial)
3. Threshold strain value can be computed according to EN 338-2016 [11] using ratio between $E_{m,90,mean}/f_{t,90,k}$ yielding 0.925e-3
4. Interpolate the point on the curve and read the actual crack length (here another criterion is added, that it happens after the first onset of nonlinear region).
5. Compute this on both sides and average the result – $a_{eopt}=a_{eoptL}+a_{eoptR}$

All the above-mentioned steps were programmed using Numpy/Scipy Python libraries.
Now when the length of crack in time is ascertained, we can do the final assessment of the optical measurement using the classic Irwin-Kies equation shown in Eq. (3). Numerically it yields:

$$G_I = \frac{P^2}{2b}\frac{\Delta C}{\Delta a_{eopt}} = \frac{P^2}{2b}\frac{\Delta \frac{u}{P}}{\Delta a_{eopt}} \qquad (10)$$

where u is the measured deflection of the sample under load P, b is the sample width and a_{eopt} is the optically measured length of crack. Note the presence of derivatives which always leads to scattered results. That is why the quantities are first smoothed using splines.

3 RESULTS

The results are summarized in Tab. 1. The values show the ones assessed using compliance-based methods (first two columns) and its graphical interpretation can be seen in Fig. 6. In the table also 5% percentile is computed, taking into account normal distribution of the results (which is in fact not absolutely ensured).
The energy denoted G_C (in some literature denoted G_{IC}, or $G_{I(PU)}$) is the resistance to crack growth at the limit load. In contrast, the critical energy release rate G_f, which takes on higher values.
A comparison of the results of compliance-based evaluation and optical measurement can be seen in Tab. 1. The authors state the value of the resistance to crack growth at the limit load in the case of optical measurement G_{copt}. The results of these two methods show good agreement for some specimens. However, the optical method generally shows higher energy values. In some cases, the difference between the results of these two methods is up to twofold.
Quantile values of energy obtained from compliance-based evaluation in comparison optical measurement show good agreement.

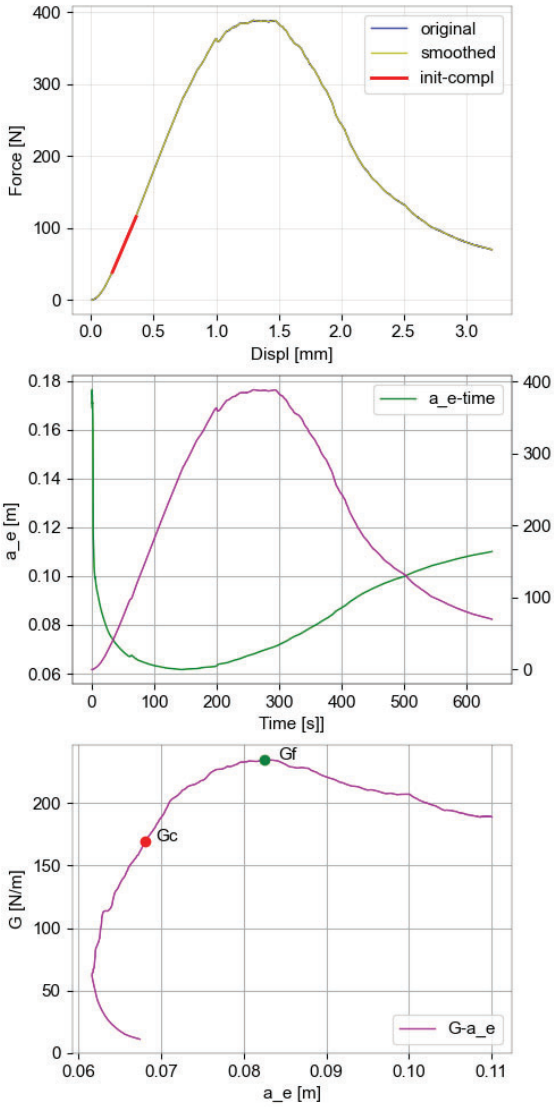

Figure 6: *Compliance-based method result of one sample: force-displacement curve with initial compliance shown in red (top), assessment of a_e (middle) and results in the form of a graph (bottom)*

It is also possible to compare the presented results with those already published, e.g., Dourado et al. [12]. It should be mentioned that the article presents the energy values of the specimens, which were calculated using the triangular stress relief region. Such a computation, to our best

https://doi.org/10.52202/069179-0022

knowledge and experience, shows similar results. The wood used to produce test specimens is the same - *Picea abies* L. The cross sections of the specimens are different (40/140 and 60/210 mm). Dourado reports a lower average wood density of 417 kg/m3 and average value of resistances to crack growth at the limit load G_c are 118 N/m for profile 40/140 mm and 106 N/m for 60/210 mm. The critical energy release rates G_f are 152 N/m (40/140 mm) and 156 N/m (60/210 mm). The published results are lower than the results in Tab. 1, more consistent with quantile values.

Table 1: *Results of the analysis*

Specimen	G_c [N/m]	G_f [N/m]	$G_c$opt [N/m]
R_007	172	238	169
R_008	184	300	264
R_009	215	258	240
R_010	171	227	270
R_011	130	211	278
R_012	170	235	185
R_013	174	229	162
R_014	167	245	219
R_015	148	217	222
R_016	144	180	211
R_017	175	241	301
R_018	156	221	288
$G_{I,mean}$	**167,2**	**233,5**	**234,1**
stdev	21,6	28,8	47,0
var.coef	0,13	0,12	0,20
$G_{I,k}$	**124,0**	**176,0**	**140,1**

It is good to discuss and mention some of the drawbacks of the method. First, of course, the threshold criterion plays an important role in the whole process. Here the authors used tabular data. Nevertheless, the nonlinear region (see Fig. 5) in the curve changes well with this criterion and looks like a reasonable one. Optical measurement is dependent on the way of smoothing the experimental data curves. The authors found that the experimental measurement does not provide a smooth flow of data. The final energy values are very sensitive precisely to the method of data smoothing.

On the other hand, the advantage of optical measurement is complete independence from other material characteristics (E_L and E_T) and also from the theory. To be exact, in compliance-based method the measured values are inserted into a very complicated model that nobody can understand directly. This is not the problem when considering the optical measurement, where the physics of the problem is clear.

Another problem is the crack length determination from two cameras. To date most SEN-TPB tests have been done without optical measurement or rather on narrower samples using DIC from one side. This is a nice contribution of the article. Actually, the difference in crack lengths on both sides was very often very high. The relatively higher values can be also attributed to the influence of this feature.

Last it should be pointed out that Dourado et al. [12] showed much lower density of timber tested, and here the authors see the biggest influence. However, the effect of different geometry of the sample could be also an important parameter.

4 CONCLUSIONS

The article summarizes the comparison of two different methods for obtaining resistance to crack growth at the maximum load. Specifically, it is a comparison of the results of compliance-based evaluation and optical measurement. The experimental work followed the methods SEN-TPB, which is basically a three-point bending with glued-in middle part, where the orientation of grain is rotated 90° to the original one.

The presented results were compared with those already published. The published results are lower than the results in this paper and are more like quantile values. It should be mentioned that the shape of the stress relief region (SRR) used in the calculation is different, but influence is not big. The cross-sections and average wood density of the samples are also different.

The quality of optical measurement results is very sensitive to the method of smoothing the experimental data curves. On the other hand, the advantage of optical measurement is complete independence from other material characteristics.

ACKNOWLEDGEMENT

This paper was created with a financial support from grant project of Grant Agency of the Czech Republic GACR No. 21-29389S “Experimental and numerical assessment of the bearing capacity of notches in timber beams at arbitrary locations using LEFM”.

REFERENCES

[1] de Moura M.F.S.F., Dourado, N.: Wood Fracture Characterization. ISBN 9780815364719, CRC Press 2018.

[2] Bažant, Z.P., Le, J.L., Salviato, M., Quasibrittle Fracture Mechanics and Size Effect: A First Course. OUP Oxford, 2021.

[3] Dourado, N., de Moura M.F.S.F., Morais, J. A numerical study on the SEN-TPB test applied to mode I wood fracture characterization, International Journal of Solids and Structures, Volume 48, Issue 2, 2011, Pages 234-242, ISSN 0020-7683.

[4] Gustafsson, P.J., A study of strength of notched beams, CIB-W18A/21-10-1.

[5] Ostapska, K., Malo, K.A., Crack path tracking using DIC and XFEM modelling of mixed-mode fracture in wood, Theoretical and Applied Fracture Mechanics, Volume 112, 2021, ISSN 0167-8442, https://doi.org/10.1016/j.tafmec.2021.102896.

[6] Coureau, Jean-Luc et al. “Cohesive zone model and quasibrittle failure of wood: a new light on the adapted specimen geometries for fracture tests.” Engineering Fracture Mechanics 109 (2013): 328-340.

[7] Oliveira, J.; Xavier, J.; Pereira, F.; Morais, J.; de Moura, M. Direct Evaluation of Mixed Mode I+II Cohesive Laws of Wood by Coupling MMB Test with DIC. *Materials* 2021, *14*, 374.
[8] Yu, Y.; Zeng, W.; Liu, W.; Zhang, H.; Wang, X. Crack Propagation and Fracture Process Zone (FPZ) of Wood in the Longitudinal Direction Determined Using Digital Image Correlation (DIC) Technique. *Remote Sens.* 2019, *11*, 1562.
[9] Xavier, J., Oliveira, M., Monteiro, P. *et al.* Direct Evaluation of Cohesive Law in Mode I of *Pinus pinaster* by Digital Image Correlation. *Exp Mech* 54, 829–840 (2014).
[10] Turner, D.Z. Digital Image Correlation Engine (DICe) Reference Manual, Sandia Report, SAND2015-10606 O, 2015.
[11] EN 338-2016 Structural timber - Strength classes, CEN Brussels, 2016.
[12] Dourado, N., de Moura M.F.S.F., Morel S., Morais, J. Wood fracture characterization under mode I loading using the three-point-bending test. Experimental investigation of Picea abies L., International Journal of Fracture, 194, 1–9, 2015.

https://doi.org/10.52202/069179-0022